Asymmetrical Planetary Nebulae II: From Origins to Microstructures
ASP Conference Series, Vol. 199, 2000
J.H. Kastner, N. Soker, & S. Rappaport, eds.

Imaging Linear Polarimetry of Proto-planetary Nebulae: the Origins of Asymmetry

Tim Gledhill, Jeremy Yates and Antonio Chrysostomou

Department of Physical Sciences, University of Hertfordshire, College Lane, Hatfield, Hertfordshire, AL10 9AB, U.K.

Abstract. It now seems likely that asymmetries in the circumstellar envelope (CSE) of intermediate mass stars develop during the latter stages of mass outflow as a star approaches the tip of the AGB. These asymmetries in the CSE must in some way give rise to the range of morphologies observed in planetary nebulae (PN) and their antecedants proto-planetary nebulae (PPN). We use imaging linear polarimetry to trace scattering in the CSEs and to reveal a morphologically diverse sample of PPN.

1. Introduction

Observations of the morphology of the CSEs in PPN can be difficult except in cases where the object is spatially well resolved, either due to its large extent or proximity, or where it appears highly elongated (bipolar) and is therefore obviously asymmetric. Bipolar PPN such as the Egg Nebula, Roberts 22 and OH 238.1+4.2 are such cases and have been well observed. Many PPN, however, appear only marginally elongated in the NIR and MIR and some are indistinguishable from PSFs in 4m telescope data. This may be due to their small angular extent so that they remain unresolved in current observations, or to geometric effects in which the main outflow axis lies close to our line of sight so that they present a smaller, symmetric profile on the sky.

Here we use NIR polarimetry to image the CSEs of a sample of PPN in scattered light. In the case of PSF-like objects, the polarimetry allows us to distinguish the polarised CSE from the underlying unpolarised photospheric component which often dominates the NIR flux.

2. Results

Imaging polarimetry was obtained at the 3.8m United Kingdom Infrared Telescope on Mauna Kea in 1998. The IRCAM3 1 $\rightarrow$ 5μm detector was used with the IRPOL2 polarisation module. The pixel scale was 0.15″and tip/tilt image correction resulted in PSFs of typically $<$ 0.5″FWHM. Objects were observed in J, H and K bands (although the data presented here are a preliminary J band reduction). The sample of 14 PPN were chosen based on the double-peaked nature of their SEDs (Kwok 1993), indicating extended CSEs, rather than on morphology. The objects are listed in Table 1.

Figure 1 shows J band linear polarisation maps of the sample of 14 PPN, superimposed on greyscale images of the J band flux. On the basis of the NIR imaging, 3 objects are clearly bipolar (16342-3814, 17150-3224 and 17441-2411) whereas the rest appear round with little evidence for elongation or deviation from a stellar PSF. However, apart from one object, 19454+2920, all objects appear highly polarised and exhibit a range of polarisation patterns. The detection of polarisation, and therefore scattered light, indicates that these objects all have spatially extended CSEs.

We categorise the objects according to their polarisation patterns as follows: *CS* - A centro-symmetric polarisation pattern with vectors arranged in a circularly symmetric fashion; *EL* - An 'elliptical' polarisation pattern where vectors deviate from centro-symmetry so that polarisations are larger along one axis than along the orthogonal axis; *AL* - An aligned polarisation pattern where all the vectors have the same orientation; *UP* - The object appears unpolarised. Out of the 14 PPN observed, 7 are EL, 4 are AL, 2 CS and 1 UP. The results are summarised in Table 1.

Table 1. A summary of the polarisation results and classification of the objects according to their morphology in total flux (column 2), their polarisation pattern (column 3) and polarised flux (column 4). Also shown are the maximum J band linear polarisation (column 5) and the position angle of the CSE symmetry axis (column 6).

Target	J Band Morph.	Pol. Pattern	Pol. Flux Morph.	$P_{max}(J)\%$	PA
16342-3814	Bipolar	AL	Bipolar	35	58
17150-3224	Bipolar	EL	Bipolar	60	128
17436+5003	Round	CS	Elongated shell?	25	275
17441-2411	Bipolar	EL	Bipolar	40	20
18095+2704	Round	EL	Bipolar?	5	105
19114+0002	Round	CS	Spherical shell?	20	0
19454+2920	Round	UP	-	-	-
19475+3119	Round	EL	Elongated shell?	30	120
19477+2401	Round	EL	Bipolar	20	205
19500-1709	Round	EL	Elongated shell?	10	92
20000+3239	Round	EL	Elongated shell?	10	34
20028+3910	Round	AL	Round	30	-
20056+1834	Round	AL	Round	15	-
21027+5309	Round	AL	Round	20	-

The distribution of linearly polarised flux (not shown) can be used to trace the regions of scattered light and hence give an indication of the geometry of the CSE (and the dust distribution). This is especially the case for objects with bright PSF-like cores, since the underlying light from the photosphere will be unpolarised. The results are again summarised in Table 1 where the objects are classified morphologically on the basis of the polarised flux distribution. It can be seen that 8 of the 11 objects that appear to be without structure in total flux do in fact have extended, elongated and sometimes bipolar CSEs. In 4 objects there is evidence for a circumstellar shell; this is most clearly seen in the case of 19114, where the shell has inner and outer radii of 1.4 and 4 arcsec respectively.

Many of the polarisation patterns are similar to those seen in Class I pre-main sequence objects which have been successfully modelled with circumstellar

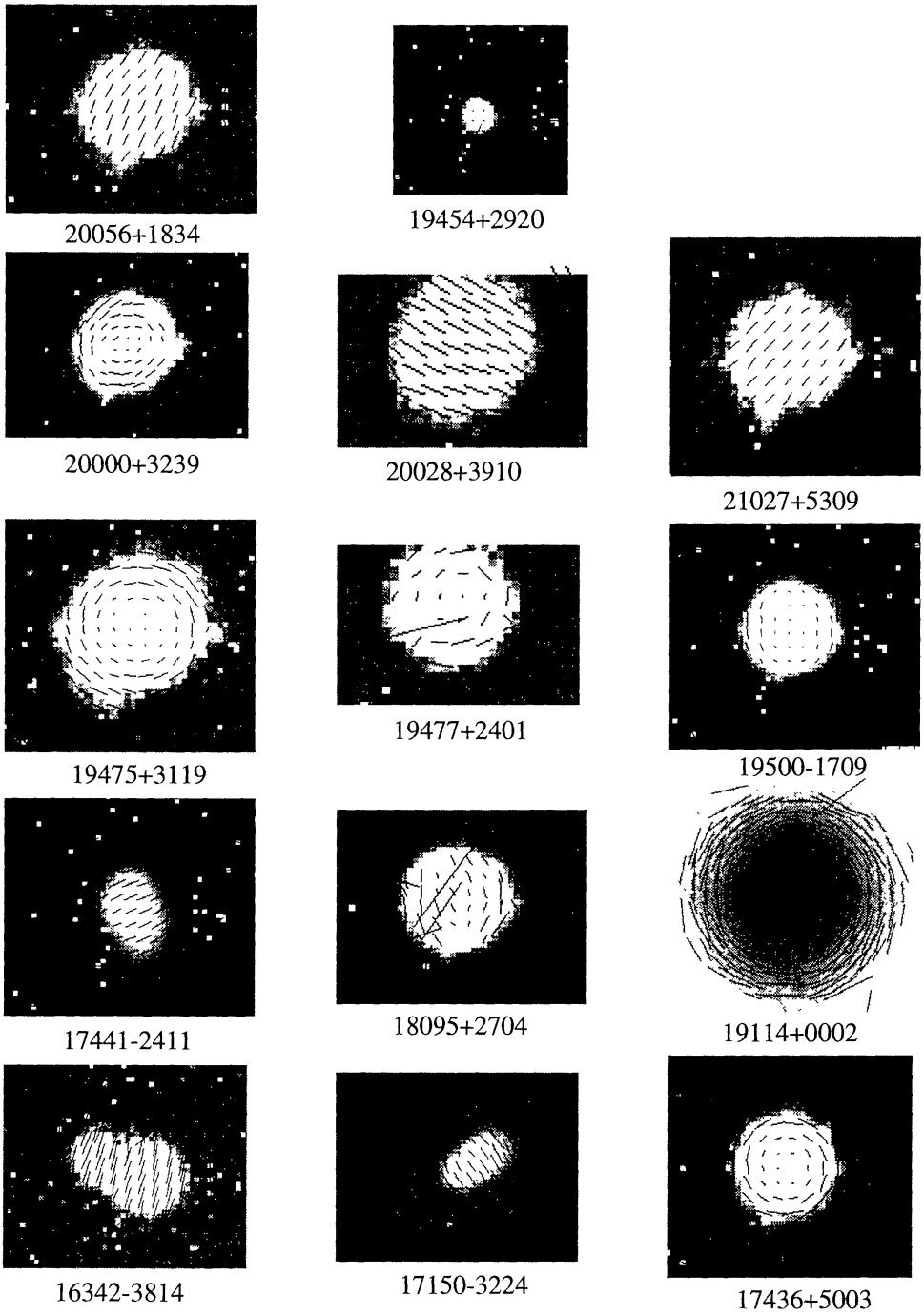

Figure 1. Linear polarisation maps superimposed on corresponding J band total flux images. North is up and East is left and the pixel scale is 0.14″. The peak polarisation levels are given in Table 1. Apart from the one unpolarised object (19454+2920), all objects show large linear polarisation and patterns indicative of scattering in extended CSEs.

discs and envelopes, where the disc provides an equatorial density enhancement, resulting in anisotropic scattering. The range of polarisation patterns then results from the angle at which the axis of the system is viewed; when the axis is in the plane of the sky, direct light from the source is obscured and light scattered in the polar lobes forms a bipolar nebula, with two distinct lobes of equal brightness in polarised flux. As the axis tilts, one lobe becomes brighter than the other due to the anisotropy of the dust scattering function with scattering angle. The polarisation pattern appears elliptical or, in the case of optically thick discs, aligned. As the inclination of the system increases, the polarisation pattern becomes more centrosymmetric. We suggest that the majority of the morphologies seen in our sample can be explained by viewing a scattering disc and envelope at various inclinations. The symmetry axes of the CSEs, defined by the polarimetry, are listed in Table 1.

Perhaps most interesting of all are the three objects that show aligned vector patterns but point source-like structure in both total and polarised flux. We suggest that these three objects are surrounded by dense axisymmetric scattering envelopes seen almost edge on, but with little or no scattering material in the polar regions, so they are not seen as bipolar nebulae. This interpretation is strengthened in the case of 20028+3910 by observations of the CO 1-0 line which show the emision elongated along an axis perpendicular to our polarisation vectors (Neri et al. 1998). Recent WFPC2 imaging of 20028+3910 also shows evidence for elongation along this axis. If the CO traces an outflow then these objects may be at an evolutionary stage where dust has yet to be ejected into the polar regions. In other words, they are about to become bipolar nebuale similar to 17150 and 17441.

3. Conclusions

Imaging polarimetry of PPN is an excellent technique for detecting the CSEs and probing the dust distribution, especially when the targets are bright and/or only partially resolved from the PSF. Imaging polarimetry of a sample of 14 PPN, chosen on the basis of their double-peaked SEDs, shows strong evidence for extended CSEs in 10 objects. Seven objects that appear 'round' in our NIR total flux images have bipolar or shell like morphologies in scattered light. Three objects show a peculiar aligned vector pattern that is difficult to reconcile with a simple scattering model. Instead they may be objects in which dust has yet to be ejected into the polar regions. Polarimetry observations of 10 of the 14 objects can be explained in terms of scattering in a disc/envelope geometry viewed at various inclinations.

References

Kwok, S. 1993, ARA&A, 31, 63

Neri, R., Kahane, C., Lucas, R., Bujarrabal, V. & Loup C. 1998, A&AS, 130, 1

Ueta, T., Meixner, M. & Bobrowsky, M. 1999, ApJ, submitted